Sustainable Structures
ISSN: 2789-3111 (Print); ISSN: 2789-312X (Online)
http://www.sustain-dpl.com/journal/sust
DOI: 10.54113/j.sust.2025.000091

ORIGINAL ARTICLE

Mechanical properties of bamboo scrimber under bolted connections with steel splints

Haitao Li[a,b,c*], Yougui Luo[a,b,c], Yijia Guo[d], Yukun Tian[a,b,c], Chungui Zhou[e], Rodolfo Lorenzo[f]

[a] College of Civil Engineering, Nanjing Forestry University, Nanjing 210037, China
[b] Jiangsu Carbon Sequestration Materials and Structural Technology of Bamboo & Wood Research Center, Nanjing Forestry University, Nanjing 210037, China
[c] National-provincial joint engineering research center of biomaterials for MACHINERY PACKAGE, Nanjing Forestry University, Nanjing 210037, China
[d] School of International Education, Tianjin Chengjian University, Tianjin 300384, China
[e] Zhejiang Runzhu Technology Co., Ltd., Hangzhou 311200, China
[f] University College London, London WC1E 6BT, UK
*Corresponding author: Haitao Li, Professor, E-mail: lhaitao1982@126.com

Abstract: Taking the bolt edge distance and spacing of bolts as the influencing factors, the tensile test of 8 groups (5 repeated groups in each group) was designed by connecting the parallel-to-grain specimens of bamboo scrimber with steel splint bolts. Based on the 5%D offset method of the American code, the key mechanical properties such as yield load and ultimate load are obtained. The test results show that the change of the bolt edge distance has little effect on the mechanical properties of the tensile specimen under the design size of the specification. The change of pitch of bolts has a significant effect on the yield load of the specimen. With the increase of spacing, the yield load and ultimate load increase gradually, reaching the maximum at 6D, and then decreasing slightly. Four typical failure modes and typical load-displacement curves of all specimen groups were analyzed. The difference between the predicted value and the experimental value in different standard calculation methods was compared. Based on the failure mode IV of double shear connection in Johansen and the cable effect and group bolt effect, the calculation formula of shear bearing capacity of steel splint bolt connection suitable for bamboo scrimber was proposed.

Keywords: Bamboo scrimber, bolted joint, steel splint, shear behavior

1 Introduction

With the current need for green building materials in structural engineering, there is an urgent need to develop and utilize new and highly reliable green building materials. According to existing research, nearly 80% of the damage to wood structures is due to connection failures at the joints of the members [1]. Therefore, it is crucial to study the reliability of joints. With the development of modern wood frame buildings towards large span and large space, the bolted connection, which is characterized by simple production, safety and reliability, high economy and fast construction, has become the main connection form in heavy and large span wood frame buildings [2,3]. The potential of bolted

Received: 16 January 2025; Received in revised form: 24 July 2025; Accepted: 20 August 2025

connections has also been fully realized in heavy timber construction. **Fig. 1** shows three ways of bolting in bamboo timber. Bamboo itself is a fast-growing, renewable natural resource [4].

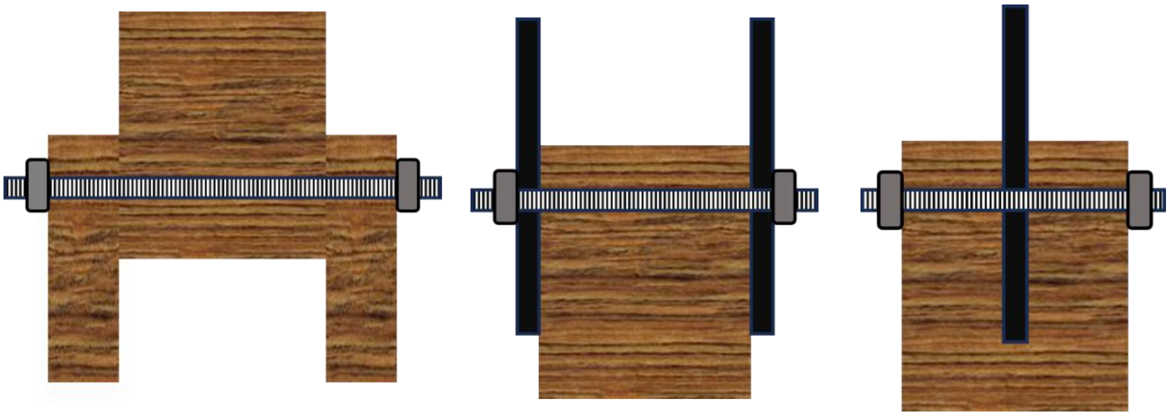

(a) Wood-wood bolted joint (b) Steel splint bolting (c) Steel filler plate bolting

Fig. 1. Types of bolted connections for bamboo and wood

Whereas, among the available building materials, the new engineered bamboo materials [5–8] and timber [9,10] meet the need for green and high reliability. Many buildings have been designed and constructed using engineered bamboo as a base material [11,12]. Among them, bamboo scrimber shows a broader engineering application prospect by virtue of its high strength-to-weight ratio. Regarding the production process of bamboo scrimber, firstly, the raw bamboo of suitable age is selected, the raw bamboo is cut and sliced, and then the bamboo slices are thinned into bamboo bundles, and then the subsequent drying, gluing and hot or cold pressing processes are carried out, among which, the hot pressing process is the traditional contact heat transfer technology, and the slab is pressed under a specific temperature, which is widely used in the process of making panels; cold pressing is the bamboo bundles dried to a certain moisture content after gluing and directly molded. The cold pressing process is to directly load the bamboo bundles which are dried to a certain moisture content after glue impregnation, and then cured and glued under high pressure, which is mostly used in the production of square materials. **Fig. 2** shows two typical bamboo scrimber projects.

(a) Bamboo house in Shangyi, Hebei (b) Bamboo toilet in Yunxi, Quzhou

Fig. 2. Bamboo scrimber projects

Many studies have been carried out on bolted connections in bamboo and wood. One of the design theories for bolted connections in wood structures was first proposed by Trayer [13], which concluded that the damage of bolted connections consists of two parts: the bending damage of the bolt and the compression damage of the substrate. Studies by other scholars [14,15] further corroborate the validity of Trayer's theory. The most widely used yield theory was proposed by Johansen [16] in 1949, which makes the bolted connections of wood structures gradually change from the design basis to the theoretical basis, in which three common damage modes of bolted steel plates and the corresponding calculation equations as well as the yield modes of double-shear bolts are introduced, which provide the basis for theoretical calculations of engineered bamboos and timbers. In the double shear connection specimen, there are four yield modes, I_m、I_s、III_s and IV of **Fig. 3**, due to the symmetric force. In the double shear connection specimen, there are four yielding modes as in **Fig. 3** due to symmetric forces. One of them, I_m, is since the compressive strength of the two side members is greater than that of the middle member, and the two side members limit the rotation of the bolt, and eventually the middle member reaches the pinned groove compressive strength and breaks. I_s is due to the connected members of the same compressive strength or both sides of the compressive strength of the members is less than the middle member, coupled with the middle member of the bolt restriction, so the two sides of the members to reach the pin groove compressive strength fc and failure; III_s is when the two sides of the members of the same compressive strength, and the middle member of the restriction of the bolt rotation, the middle member of the plastic hinges; damage mode IV is when all the members of the compressive strength is greater, bolt will produce plastic hinges in all members. Daudeville [17] and Yasumura [18] investigated the failure forms of bolted joints in timber, considering the factors of pin diameter, margin, and end moments, and the results showed that the bolt diameter has an effect on the pin groove compression strength, which can be improved by increasing the bolt diameter when the margin and end moments are below the minimum values. Mohammad [10] conducted a study on the performance of steel-wood bolted joints and suggested that the Canadian standards are too conservative and not optimal for assessing the load carrying capacity of wood and proposed an alternative design method for predicting the damage modes and ultimate strengths of steel-wood-steel bolted joint combinations. Cabrero [19] evaluated the performance of an existing model and found that ductile damage could be achieved by satisfying the minimum spacing between fasteners. Li [20] conducted a more comprehensive study on the compressive properties of bamboo-steel bolted joints and found that the loads obtained from the tests were higher than the corresponding theoretical values in the national codes. There is a lack of research on the tensile properties of bolted connections of bamboo scrimber in the existing models.

(a) I_m **(b) I_s** **(c) III_s** **(d) IV**

Fig. 3. Yield mode of a double shear connection

As discussed above, few studies about the tensile properties of bolted joints with bamboo scrimber has been carried out. However, tensile stress is common in the bolted joints. It is meaningful to investigate the mechanical properties of bolted joints of bamboo scrimber. Thus, a series of tensile tests about bolted steel-bamboo-steel connections loaded parallel to grain are studied in this paper considering various influencing factors. The failure modes and bearing capacity of the joints are studied.

2 Materials and Methods

2.1 Materials

The bamboo scrimber material used in this experiment was produced and supplied by Hangzhou Run Bamboo Technology Co., Ltd. Moso bamboo harvested with the age of 3 to 5 years was selected from Fujian province. The raw materials were cut into length of 1930 ± 20 cm and were broken into bamboo culms that could be crushed into bamboo bundles, with a width of 4-8 cm. Then all bamboo culms were dissembled into bamboo fiber bundles after removing the green surface and inner yellow parts. Finally, the process of glue impregnation and hot pressing in a 400-t press at 115-135 ºC, followed by maintenance, the required raw materials of bamboo scrimber were gained. Due to the limitation of the mold, the thickness of the hot-pressed sheet is 50 mm, so the sheet exceeding this thickness needs to be cold-pressed twice, but the thickness of the specimens used in this test is not more than 50 mm. Following "Test Method for Physical and Mechanical Properties of Bamboo Materials for Construction" [21] and ASTM-D143-14 [22] , the material properties of the bamboo scrimber as well as the bolts were tested, and the results are shown in **Table 1**.

Table 1 Material properties of bamboo scrimber

	Bamboo scrimber				Q235 bolts				
	Compression	Tensile	Shear	Parallel dowel bearing strength (MPa)	Compression (MPa)	Tensile (MPa)	Flexural (MPa)	Density (g/cm^3)	Water content (%)
Strength (MPa)	129.19	140.56	20	143.19	235	188	610.37	1.151	6.60
Elastic modulus (MPa)	14151	13398	4646						

2.2 Methods

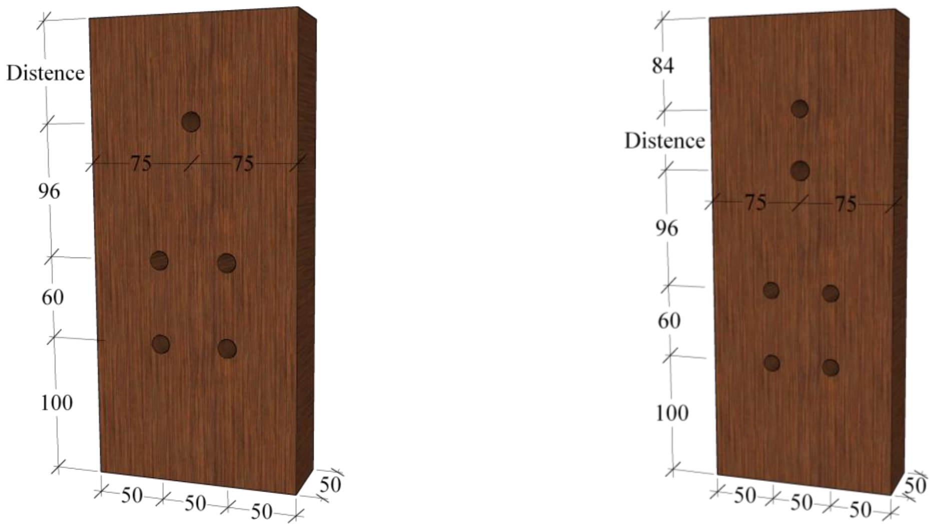

(a) Bolt edge distance (b) Pitch of bolts

Fig. 4. Schematic diagram of specimen (Unit: mm)

Table 2. Specimen parameters

Influencing factors	Groups	Bolt diameter (mm)	Distance (mm)	Specimen size (mm)		
				Length	width	Thickness
Bolt edge distance	ZPTB6D	12	72	328	150	50
	ZPTB7D		84	340	150	50
	ZPTB8D		96	352	150	50
	ZPTB9D		108	364	150	50
Spacing of bolts	ZPTB2×1-4D		48	388	150	50
	ZPTB2×1-5D		60	400	150	50
	ZPTB2×1-6D		72	412	150	50
	ZPTB2×1-7D		84	424	150	50

Note: To ensure that the specimen and the bolt can be installed accurately, the actual diameter of the punched hole is 1.5 mm larger than the diameter of the bolt.

The test was designed with 4 groups of single bolts with different margins, 4 groups of double bolts with different spacing, and 8 different connection configurations for the tensile test. Each group contains 5 identical specimens and the total number of the specimens is 40. Detailed information about the specimens are shown in **Fig. 4** and **Table 2**. All the specimens were punched with a diameter of 13.5 mm (to reserve part of the gap to ensure that the bolts can be put into the holes), the bolts used in the test were Q235 steel with a diameter of 12 mm, and the steel clamp plate was Q345 alloy steel with a thickness of 10 mm. The schematic diagram of specimen loading is shown in **Fig. 5**. 200 t microcomputer controlled electro-hydraulic servo universal testing machine was chosen and TDS-530 was used to collect data. The test loading speed was 1 mm/min, and was stopped when the test specimen was damaged or the load decreased to 70% of the maximum value. Before the start of the test, the four surfaces of the specimen were numbered A, B, C, and D. The specimen was assembled with the steel plate by bolts, and then the two ends of the steel plate were fixed by the clamping end. Three displacement gauges were used to measure the displacement, one was placed under the pallet to measure the beam displacement, and the other two gauges were placed against the adhesive iron sheet on the lower part of the main member to measure the relative slip between the bamboo scrimber member and the steel plate, and all the data collected by the system were saved to a personal computer.

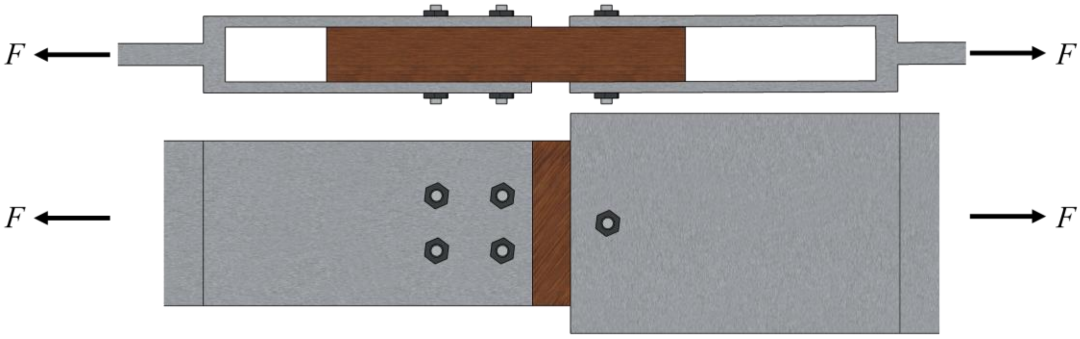

Fig. 5. Schematic diagram of specimen loading

3 Test results and analysis

3.1 Mode of failure

According to the damage form of the specimen and the characteristics of the load-displacement curves, both single-bolt and double-bolt connection specimens can be divided into two typical damage modes. The typical damage modes of single bolt and double bolt are shown in **Fig. 6** and **Fig. 7.**

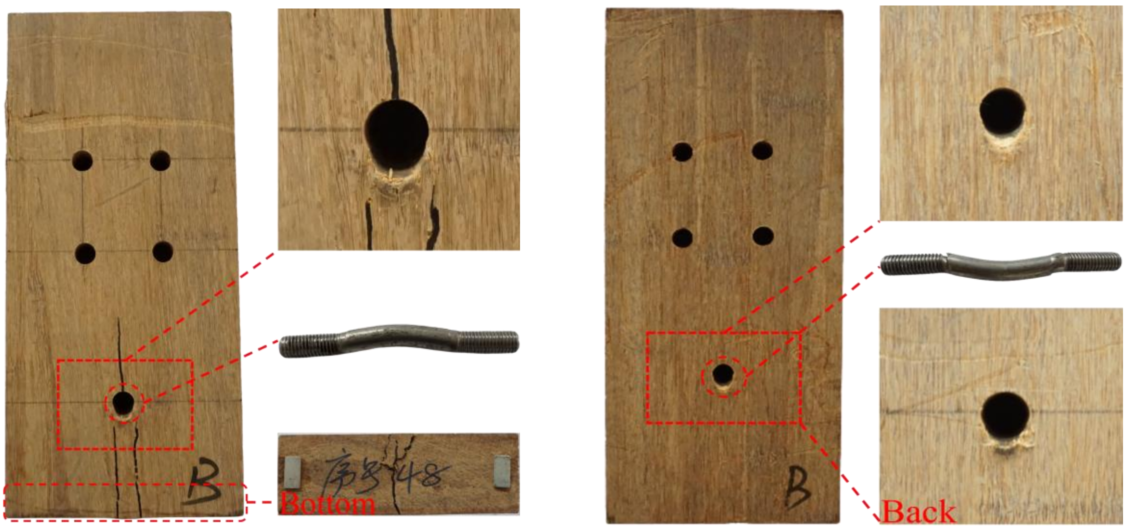

(a) Failure mode I (b) Failure mode II

(c) Bolt group photo

Fig. 6. Single bolt damage pattern

3.1.1 Failure mode I of single bolt

As for failure mode I of single bolt, seen from **Fig. 6(a)**, bamboo fiber tearing sound could be heard soon in the initial loading stage. With the increase of the load, obvious bending deformation could be seen for the single bolt accompanied with bamboo fiber fracture sound and cracks along the bolt holes extended upward and exceeded the height of the steel splint. With the load close to the ultimate load value, bamboo fiber fracture sound continued until the main component cannot bear load. After removing the steel splints, cracks were formed at the bottom of the bolt holes in the specimen due to the compression of the bolts. Some bamboo materials were pushed put by the bolt and we named it as shear compression failure mode which occurred in the specimen with small edge distance. This mode is ductile damage and it occurred as shear splitting that progressively developed along the crack because of insufficient strength of the main component due to the small margins of the bolt holes.

3.1.2 Failure mode II of single bolt

As can be seen from **Fig. 6(b)** for failure mode II of single bolt, the bolt is sheared and the bolt hole is crushed which always occurred in the specimens with large side distances. No obvious fiber tearing sounds were produced during the loading process of the main components, nor were there any obvious component damage phenomena. When the load was close to the ultimate load, the ends of the bolts would suddenly be cut off, and the nodes could no longer bear the load. After the test was completed and the steel plate was removed, it was found that there were no obvious cracks in the main components. The bolt holes had obvious deformation caused by the compression of the bolts, and the ends of the bolts had shear fracture, which was a shear failure of the bolt ends due to insufficient strength of the bolts. As for the bamboo scrimber base material, there was a phenomenon of crushing at the bolt openings. This was caused by the excessive pitch of the bolt holes and insufficient strength of the screw.

Typical damage schematics of the bolts in the above two damage modes are shown in **Fig. 6(c)**, and all the bolts exhibit a distinct double-hinge yield mode.

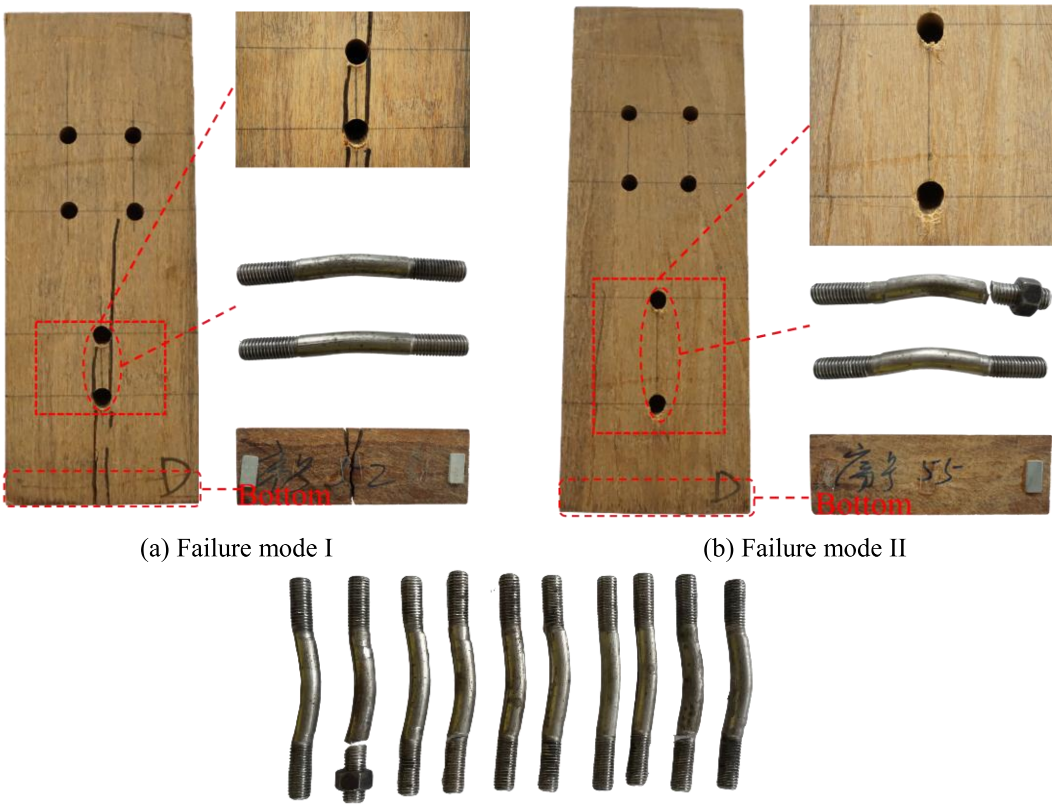

(a) Failure mode I
(b) Failure mode II

(c) Bolt group photo

Fig. 7. Double bolt damage pattern

3.1.3 Failure mode I of double bolts

This failure mode always occurred in the specimen group with smaller bolt spacing. Fiber fracture sound could be heard continuously in the main component bolt hole location in the beginning of loading. With the increasing of the load, clear cracks appeared and extended upward and over the range of the steel plate, accompanied by the crisp sound of the main component, the joint cannot continue to carry load. After removing the steel plate when the test was finished, the development of the cracks could be seen clearly. It could be observed that the cracks extended from the bolt hole to the loading direction. In the beginning, the cracks along the bolt hole developed simultaneously. And then a penetrating crack appeared between the two bolt holes. When the cracks continued to develop in the extension direction, they converted into a main crack and extended to the clamped end of the main component. The downward-developing cracks penetrated through the bottom of the whole main member and pushed out the end part of the bamboo materials in a shear manner. There was a significant extrusion deformation of the bolt holes, and the bolts were in the double-hinged yielding mode. This damage mode belongs to the damage mode of end shear push-out, seen from **Fig. 7(a)**.

3.1.4 Failure mode II of double bolts

As for this failure mode, it always occurred in the specimens with large bolt spacing. Non obvious damage phenomenon during the whole test could be found, and the specimen cannot be loaded because of the end shear damage of the bolt. As can be seen from Fig. 7(b), after removing the steel plate, the bolt holes have obvious traces of extrusion, and the bolt appeared single-hinged yielding and was cut off by the end of the steel plate. The main components did not fully utilize the tensile properties of the materials, and the utilization of the material was limit in the specimens with larger bolt spacing. Shear damage of the bolt occurs in the bolt farther from the loading end. It is suggested that the strength grade of bolts farther away from the loading end can be upgraded in the specimen group with larger bolt spacing.

Fig. 7(c) shows the typical damage patterns of bolts, and most of the bolts belongs to double hinged failure. As the bolt spacing increases in the double bolt specimens, the degree of bolt bending increases.

3.2 Load displacement curve

Fig. 8 shows the load-displacement curves of the typical specimen group of bamboo scrimber-steel splint bolted joints under tension along the grain (the gray dotted line is the test curve, and the red solid line is the average curve). Seen from **Fig. 8**, the bolt has about 2 mm free slip at the beginning of loading in the curves. As for the single bolt joint, when the load was increased to about 10 kN, the bolt and the main member bolt hole were completely contacted. The load displacement increased linearly, and the joint entered into linear elasticity stage. While for the double-bolt joint, it entered into linear elasticity stage when the load was increased to 20 kN. And the breakage of the bamboo fiber occurs in some of the test specimens during this process. When the load was increased to about 80 kN and 140 kN respectively, the load growth trend of single-bolt joints and double-bolt joints decreased significantly, and a small yielding platform appeared in single bolt joints, while there was no obvious yielding stage in double bolt connection joints. When the load value was 80 kN for the single bolt joint, the load decreased suddenly due to the bottom of the main member being pressed out by the bolt or the end of the bolt being cut off by the steel cleat. When the load value for the double bolt specimen with the spacing of 7*D* reached 160 kN, the joint cannot continue to be loaded because the end of the bolt was sheared by the steel plate. The load decreases and the joint is damaged. From the load displacement curve, the tensile damage of the double bolt joint is a brittle damage that occurred suddenly, and the type of tensile state of the ZPTB2×1-6D double bolt joint should be avoided in the actual project.

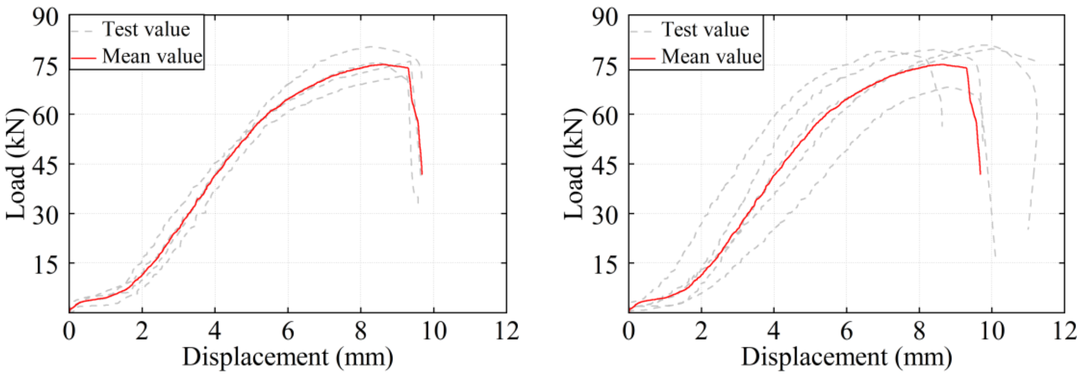

(a) ZPTB6D (b) ZPTB7D

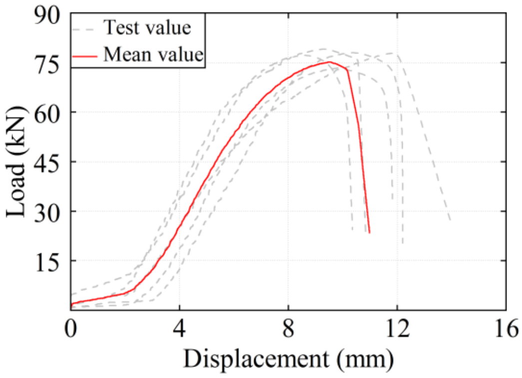

(c) ZPTB8D

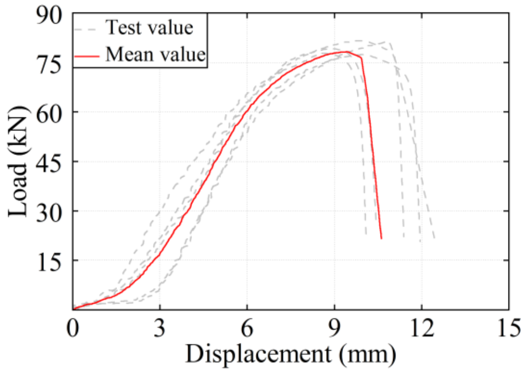

(d) ZPTB9D

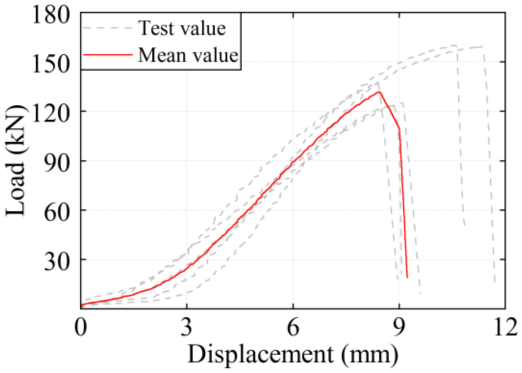

(e) ZPTB2×1-4D

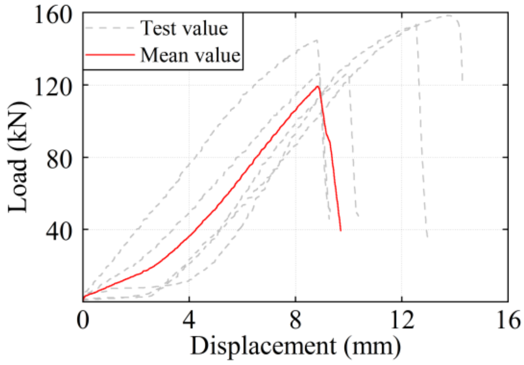

(f) ZPTB2×1-5D

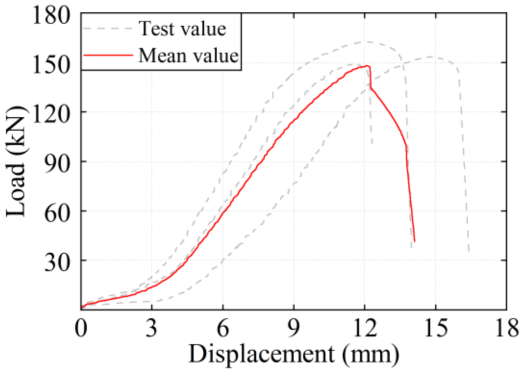

(g) ZPTB2×1-6D

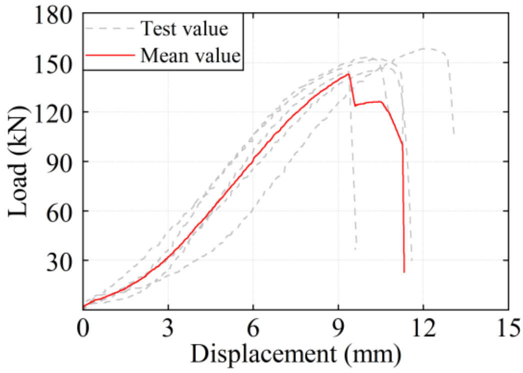

(h) ZPTB2×1-7D

Fig. 8. Single bolt load displacement curve

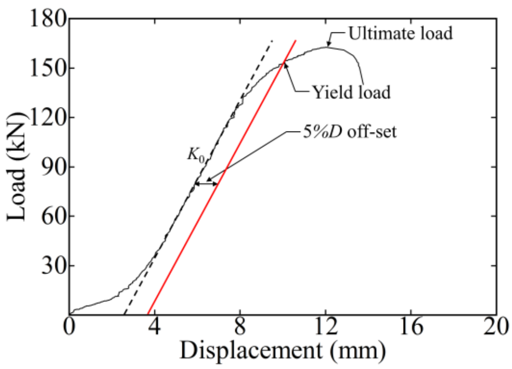

Fig. 9. 5%D displacement value method

3.3 Analysis of key mechanical properties

The test results were taken using the 5%D displacement method in ASTM D5764-97a [23]. As shown in **Fig. 9**, the stiffness value of the specimen in the elastic phase was first obtained, and then this oblique straight line was moved to the right by 5%D. The load value at the intersection with the load displacement curve was the yield load (D is the bolt diameter).

The test results of single bolt and double bolts connection joints of bamboo scrimber-steel splint are shown in **Table 3**. Seen from **Table 3**, with the increasing of the bolt edge distance for the single bolt groups and the spacing for double bolts groups, most of the related average values shown in the table increased overall except the initial stiffness (K). However, the increasing trend is clearly for the average yield values of yield load (P_y) and ultimate load (P_u), but not for the average values of yield displacement (d_y), ultimate displacement (d_u), and ductility ratios (μ).

Table 3 Test results of single-bolt and double-bolt joints

Groups	P_y (kN)	P_u (kN)	K (kN/mm)	d_y (mm)	d_u (mm)	μ
ZPTB6D	65.37 (4.60)	76.08 (4.10)	15.87 (6.64)	7.23 (8.82)	10.70 (6.65)	1.48 (2.50)
ZPTB7D	69.05 (4.78)	77.63 (6.05)	18.38 (8.26)	6.66 (20.11)	10.35 (11.30)	1.60 (15.20)
ZPTB8D	68.81 (4.14)	82.66 (2.88)	14.85 (8.07)	7.69 (10.57)	11.97 (12.45)	1.57 (12.05)
ZPTB9D	70.59 (7.39)	79.62 (2.17)	15.49 (16.06)	7.67 (11.34)	11.75 (12.21)	1.54 (8.06)
ZPTB2×1-4D	128.26 (3.76)	131.62 (4.57)	22.09 (8.17)	8.63 (5.81)	10.05 (10.85)	1.16 (7.64)
ZPTB2×1-5D	137.58 (7.53)	142.21 (9.19)	20.94 (11.61)	10.10 (15.26)	11.25 (18.16)	1.11 (6.90)
ZPTB2×1-6D	149.63 (2.12)	155.31 (3.54)	20.01 (14.59)	11.50 (17.66)	14.24 (11.82)	1.26 (11.47)
ZPTB2×1-7D	146.36 (3.16)	151.23 (3.13)	21.37 (2.63)	9.40 (0.94)	11.28 (1.11)	1.20 (0.59)

Note: Within brackets is the coefficient of variation (%).

3.3.1 Bolt edge distance effect

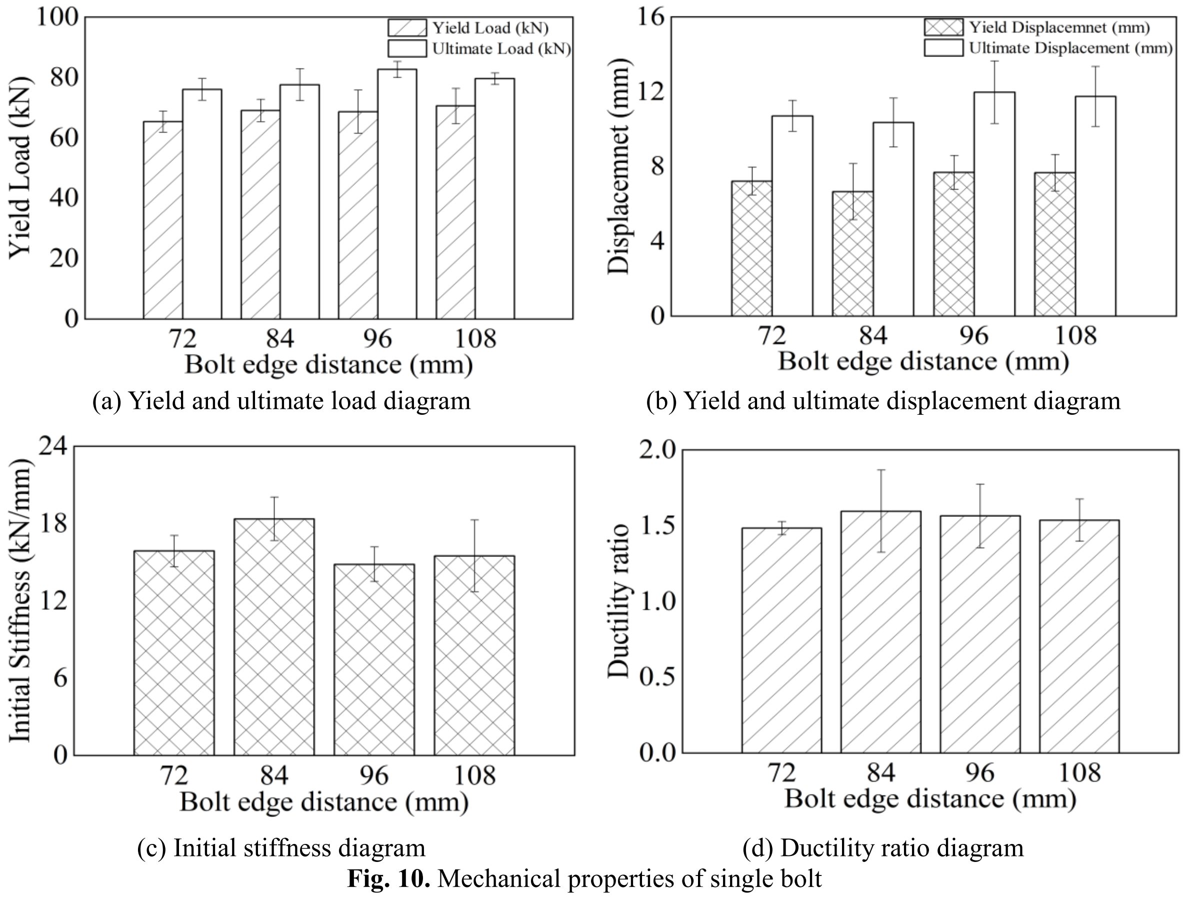

(a) Yield and ultimate load diagram (b) Yield and ultimate displacement diagram

(c) Initial stiffness diagram (d) Ductility ratio diagram

Fig. 10. Mechanical properties of single bolt

As can be seen from **Fig. 10**, the yield load and ultimate load of the single bolt specimens appear to increase and then stabilize with the increase of the side distance of the bolt, and even the ultimate load appears to decrease slightly with the increase of the side distance and reaches 8*D*. The initial stiffness tend to stabilize with the increase of the side distance, in which the difference between the maximum and minimum values of the initial stiffness is 15.47%. Both the yield displacement and ultimate displacement reach the maximum value at 8*D*. The initial stiffness tend to be stable with the increase of side distance, in which the difference between the maximum and minimum values of the initial stiffness is 15.47%. The increase for the ductility ratio is not clear, and the difference between the maximum and minimum values of the ductility ratio is 8.11%.

3.3.2 Spacing of bolts effect

Fig. 11 shows the bolts spacing effect for the specimen with double-bolt connection. With the increase of bolt spacing, the yield load and ultimate load increased gradually and reach the maximum value at 6*D*, and then decreased slightly to keep stable. The yield and ultimate displacements reached their maximum values at 6*D*, and a sudden decrease occurs when the spacing was increased. The initial stiffness and ductility ratios remained stable with the change of spacing.

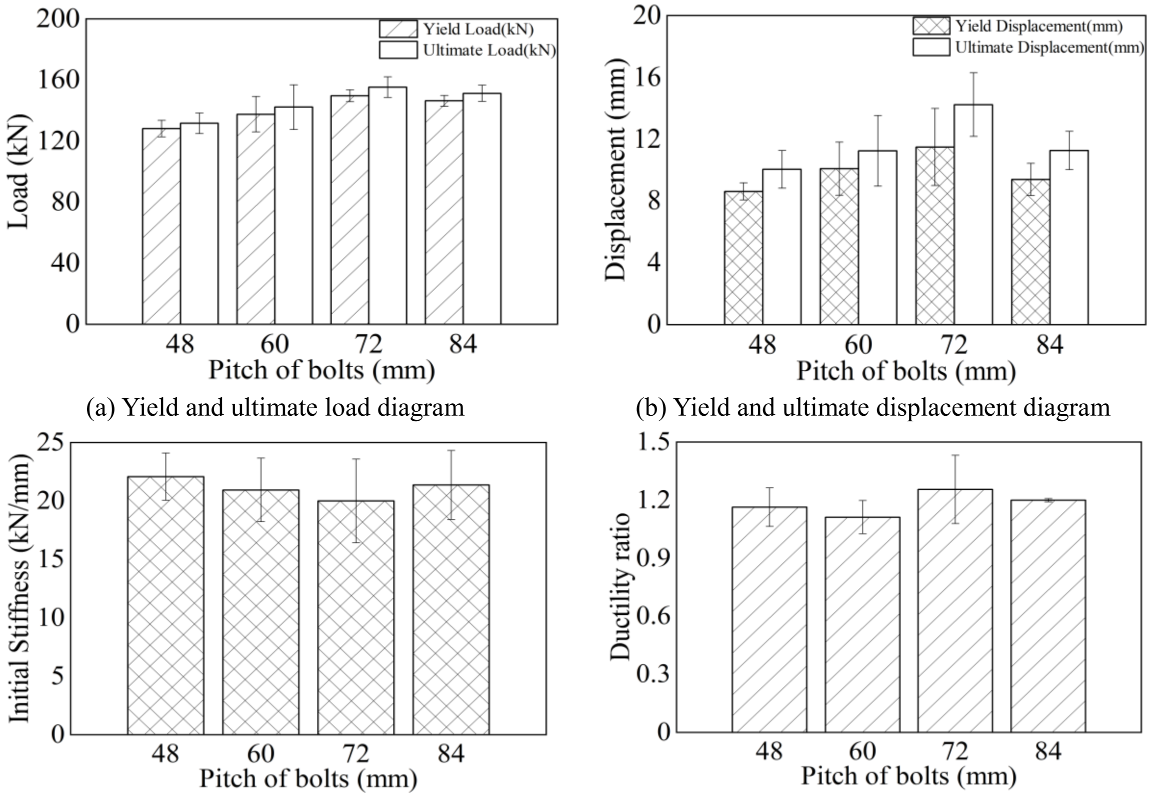

(a) Yield and ultimate load diagram (b) Yield and ultimate displacement diagram

(c) Initial stiffness diagram (d) Ductility ratio diagram

Fig. 11. Mechanical properties of double bolt

The single bolt specimen maintains a higher ductility ratio and lower stiffness and strength compared to the double bolts specimen. With the increase in the number of bolts, the forces on the individual bolt were spread out, and the load carrying capacity of the multi-bolt specimen increased. The failure for the specimen were transformed from plastic damage to brittle damage. In the double bolts specimen, the load carrying capacity of the specimen did not continue to increase as the spacing increases. There was a maximum at a certain value, and then decreased slightly and remains stable.

4 Calculation of load capacity

4.1 Analysis of the applicability of the current formula

According to the double hinge yield mode of the bolt in this paper, which is the IV mode in **Fig. 3**, the theoretical load is obtained by taking the bearing capacity calculation formula of the corresponding failure mode in each specification.

4.1.1 NDS[24]

The American code revised the shear capacity of bolts in 1991 and introduced the safety factor R_d based on Johansen theory. When the failure mode of the bolt is IV, the shear capacity of the bolt of the double shear connection is calculated according to the following formula.

$$F = \frac{D^2}{R_d}\sqrt{\frac{2F_{em}F_{yb}}{3(1+R_e)}} \tag{1}$$

$$R_d = 3.2k_\theta \tag{2}$$

In the formula, $R_e=F_{em}/F_{es}$; $R_t=t_m/t_s$; F_{es} is the design value of the compressive strength of the side member holes and grooves is 1.1 times that of Q345 steel, which is 379.5 MPa [25]; F_{em} is the design value of the compressive strength of the main member hole groove; The t_m is 50mm thick for the main member; t_s is a side member thickness of 10mm; F_{yb} is the bending yield strength of the bolts; D is the diameter of the bolts (12mm); and $k_\theta=1+\theta/360$, where θ is the angle between the load and the smooth grain of the wood.

4.1.2 CSA[26]

When the damage mode of the bolt is IV, the shear bearing capacity of the bolt is calculated according to the following formula.

$$F_v = 0.8f_{es}d^2\sqrt{\frac{2}{3}\frac{f_{em}}{(f_{es}+f_{em})}\frac{f_y}{f_{es}}} \tag{3}$$

In the formula, f_{es} is the pin groove compressive strength of the side member; f_{em} is the pin groove compressive strength of the main member; d is the bolt diameter; t_s is the thickness of the side member; f_y is the bending yield strength of the bolt.

4.1.3 Eurocode 5[27]

When the failure mode of the bolt is IV, the shear bearing capacity of the single shear and double shear connection is calculated according to the following formula.

$$Z = 1.05\sqrt{\frac{2\beta}{1+\beta}}\sqrt{2M_{y,RK}f_{es}d} + \frac{F_{ax,Rk}}{4} \tag{4}$$

$$\beta = f_{em}/f_{es} \tag{5}$$

In the formula, t_s is the thickness of the side member; the bearing strength of the pin groove of the main component of the f_{em}; f_{es} is the compressive strength of the pin groove of the edge member; $M_{y,RK}$ is the bending yield moment value of bolt fasteners; d is the bolt diameter; $F_{ax,Rk}$ is the characteristic value of bolt pullout.

Cui [28] proposed in his article that M_y in the NDS [24] specification is closer to the experimental value than other specifications.

$$M_y = k_w W f_{yb} \tag{6}$$

In the formula, k_w is the ratio of the plastic section modulus to the elastic section modulus of the section. Due to the full section yield of the circular bolt, the plasticity of the material is fully developed, which can be taken as 1.7; W is the torsional section modulus; f_{yb} is the bending yield strength of the bolt.

4.1.4 GB/T50005-2017[29]

In the Chinese code, the shear bearing capacity of a single bolt is calculated according to Eq. (9) in the single shear connection and symmetrical double shear connection of bolts.

$$Z = k_{\min} t_s d f_{es} \tag{7}$$

$$k_{\min} = \min\{k_{\mathrm{I}}, k_{\mathrm{II}}, k_{\mathrm{III}}, k_{\mathrm{IV}}\} \tag{8}$$

$$k_{\mathrm{IV}} = \frac{d}{1.88 t_s}\sqrt{\frac{1.647 R_e f_{yk}}{3(1+R_e) f_{es}}} \tag{9}$$

In the formula, $R_e = f_{em}/f_{es}$, t_s is the thickness of the side member; the bearing strength of the pin groove of the main component of the f_{em}; f_{es} is the compressive strength of the pin groove of the edge member; k_{min} is the minimum effective length coefficient of bolt hole bearing pressure, according to the yield mode of different bolts; d is the bolt diameter; f_{yk} is the standard value of yield strength of bolt fasteners.

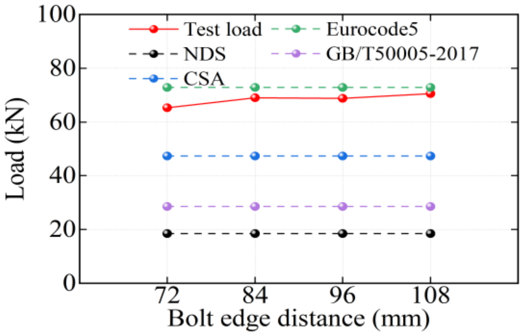

(a) Single bolt

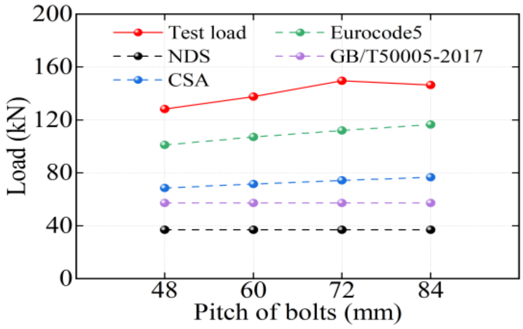

(b) Double bolt

Fig. 12. Comparison of theoretical and test loads in different standards

Table 4 Comparison of theoretical and test loads in different standards

Groups	Test load (kN)	Theoretical load (kN)			
		NDS	CSA	Eurocode 5	GB/T50005-2017
ZPTB6D	65.37	18.51	47.39	72.85	28.58
ZPTB7D	69.05	18.51	47.39	72.85	28.58
ZPTB8D	68.81	18.51	47.39	72.85	28.58
ZPTB9D	70.59	18.51	47.39	72.85	28.58
ZPTB2×1-4D	128.26	37.03	68.43	101.25	57.17
ZPTB2×1-5D	137.58	37.03	71.55	107.06	57.17
ZPTB2×1-6D	149.63	37.03	74.21	112.05	57.17
ZPTB2×1-7D	146.36	37.03	76.53	116.45	57.17

The predicted strength of bamboo scrimber bolted joints in different specifications is shown in **Table 4** and **Fig. 12**. The shear prediction formulas of NDS, CSA and GB/T50005-2017 are too conservative in this test, and the predicted load of Eurocode 5 is closest to the test load. Therefore, the calculation method of this test will be based on the Johansen yield model used in Eurocode 5.

4.2 Construction of computational methods

In the calculation of bearing capacity of bolt nodes of bamboo and wood structures, based on the Danish scholar Johansen [16] assumed that the pin groove bearing curve for the ideal stiffness-plasticity relationship is the most widely used theoretical model at present, and different calculation methods for different yield modes have been proposed and adopted by the design codes of other countries [24,26,27]. Therefore, this paper is based on Johansen's yield mode IV, and combined with the experimental phenomenon to reorganize the bamboo bolt node connection of the construction of the calculation method.

4.2.1 Analysis of Johansen yield mode

From the failure mode, the bolt used in this test is double hinge failure, and the stress distribution of the connector is analyzed by taking the specimen with double hinge yield on the right side of a single bolt, as shown in **Fig. 13**.

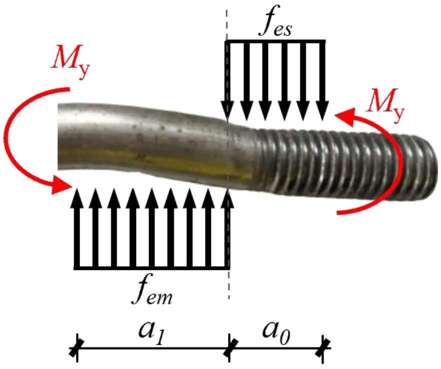

Fig. 13. Connector stress distribution diagram

According to the balance of forces, $\sum F_y=0$, it can be obtained:

$$F_v = f_{es} d a_0 = f_{em} d a_1 \tag{10}$$

$$a_0 = \beta a_1 \tag{11}$$

Based on the moment equilibrium, $\sum M=0$, the moment is solved for the left plastic hinge:

$$2M_y = f_{es} d a_0 (a_1 + \frac{a_0}{2}) - f_{em} d a_1 \frac{a_1}{2} \tag{12}$$

Simplifying Eq. (12) gives:

$$a_1 = 2\sqrt{\frac{M_y}{(1+\beta) d f_{em}}} \tag{13}$$

$$a_0 = \beta a_1 = 2\beta\sqrt{\frac{M_y}{(1+\beta) d f_{em}}} \tag{14}$$

$$F_v = f_{es} d a_0 = f_{em} d a_1 = 2\sqrt{\frac{M_y d f_{em}}{(1+\beta)}} \tag{15}$$

In the formula, F_v is the single shear surface bearing capacity of a single bolt; f_{es} is the pin groove bearing strength of the side member; d is the bolt diameter; α_0 is the pin groove bearing strength of Q345 steel; f_{em} is the pin groove bearing strength of the main member; α_1 is the reorganization of the pin groove bearing strength of the bamboo; $\beta=f_{em}/f_{es}$; M_y is the value of bending yielding moment of the bolt fasteners.

4.2.2 Rope effect

According to the consideration of rope effects in Eurocode 5, for the tests in this paper $F_{ax,Rk}/4$ should be taken, and the limit of the role of rope effects on the load carrying capacity when the connection is a bolt should be within 25% of Johansen's part, where $F_{ax,Rk}$ is the characteristic pull-out load carrying capacity of the fastener. After considering the rope effect, the bearing capacity F_v of a single shear surface of a single bolt connection is:

$$F_v = 2\sqrt{\frac{M_y d f_{em}}{(1+\beta)}} + \frac{F_{ax,Rk}}{4} \tag{16}$$

In the formula, $F_{ax,Rk}$ is the characteristic value of bolt pullout resistance.

4.2.3 Group-bolt effect

When multiple bolts work together, the force of each bolt is not the same, and the total bearing capacity is not a simple numerical superposition. Therefore, the determination of the number of effective bolts in Eurocode 5 is the key to predict the performance of bolted joints.

Table 5 Number of effective bolts in tension along grain

Groups	Spacing (mm)	n_{ef} test value	n_{ef} theoretical value			
			Eurocode 5	Error (%)	Test	Error (%)
ZPTB2×1-4D	48	1.86	1.06	-33.83	1.89	1.72
ZPTB2×1-5D	60	1.99	1.19	-35.42	1.98	-0.56
ZPTB2×1-6D	72	2.17	1.30	-41.08	2.05	-5.72
ZPTB2×1-7D	84	2.12	1.41	-32.62	2.12	0.15

In this test, the edge distance of ZPTB7D is the same as that of the other double bolt specimens. Taking ZPTB7D as the bearing capacity of single bolt Fu1 and substituting it into Eq. (17), the nef test value is obtained, which is shown in **Table 5**.

$$n_{\mathrm{ef}} = F_{\mathrm{u}} / F_{\mathrm{u1}} \tag{17}$$

$$n_{\mathrm{ef}} = n_{\mathrm{r}} n^{0.9} \sqrt[4]{\frac{a_1}{13d}} \tag{18}$$

In the formula, n_r is the number of bolt columns; n is the number of bolts per column; α_1 is the row spacing; F_u is the total bearing capacity of the bolt; F_{u1} is the bearing capacity of single bolt.

Theoretical effective number of bolts n_{ef} derived from the substitution of Eq. (18) and the test value comparison results shown in **Table 5**, the theory is conservative, and the test value of the error is large. This is due to the number of effective bolts in the original standard is based on the wood as the main member, when the bolt occurs a small deformation is the main member of the bolt hole is crushed and loss of load-bearing capacity. Bamboo scrimber, as an engineered bamboo material, has a much greater pinning strength than ordinary wood, so it is necessary to construct a formula for the number of effective bolts with a higher degree of fit. CSA [26] proposed an effective bolt formula based on the results of Zahn [30] and considering the effects of row spacing, thickness-to-diameter ratio, and the number of bolt rows:

$$n_{\mathrm{ef}} = 0.33\left(\frac{t}{d}\right)^{0.5}\left(\frac{s}{d}\right)^{0.2} n^{0.7} \tag{19}$$

In the formula, t is the thickness of the main member; d is the bolt diameter; s is the row spacing; n is the number of rows of bolts (this paper takes 2).

Because the thickness-diameter ratio of this specimen is a fixed value, the calculation model is simplified as follows:

$$n_{\mathrm{ef}} = a_1\left(\frac{s}{d}\right)^{a_2} 2^{a_3} \tag{20}$$

Through regression analysis, the formula for calculating the number of effective bolts of the bolted joints of the bamboo scrimber steel splint is:

$$n_{\mathrm{ef}} = 0.9\left(\frac{s}{d}\right)^{0.2} n^{0.7} \tag{21}$$

It can be seen from the table that the maximum error between the number of effective bolts predicted by Eq. (21) and the experimental value is -5.72%, which proves that the formula is reliable.

In summary, after considering the group bolting effect, the formula for the shear capacity of the bolted node of the bamboo scrimber steel splint, F_v can be expressed as follows:

$$F_{\mathrm{v}} = \left(2\sqrt{\frac{M_y d f_{\mathrm{em}}}{(1+\beta)}} + \frac{F_{\mathrm{ax,Rk}}}{4}\right) n_{\mathrm{ef}} \tag{22}$$

$$n_{\mathrm{ef}} = \begin{cases} 1 & n = 1 \\ 0.9(s/d)^{0.2} n^{0.7} & n \geq 2 \end{cases} \tag{23}$$

Table 6 Comparison of test load with theoretical load

Number	Test load (kN)	Theoretical load (kN)	Error (%)
ZPTB6D	65.37	69.91	6.49
ZPTB7D	69.05	69.91	1.23
ZPTB8D	68.81	69.91	1.57
ZPTB9D	70.59	69.91	-0.98
ZPTB2×1-4D	128.26	132.31	3.06
ZPTB2×1-5D	137.58	138.35	0.56
ZPTB2×1-6D	149.63	143.49	-4.28
ZPTB2×1-7D	146.36	147.98	1.09

As can be seen from **Table 6**, the error between the theoretical load and the test load ranges from -4.28% to 6.49%, indicating that the shear capacity equations for the bolted nodes of the bamboo scrimber steel splints constructed in this paper on the basis of Johansen's yield mode IV and the rope effect and the bolt effect accurately describe the relationship between the bolt spacing and the bearing capacity of the single-bolt connection as well as the multi-bolt connection.

5 Conclusions

In this paper, the tensile properties of the bolted joints of steel splints were tested for the parallel-grain specimens of bamboo scrimber. The 5%D displacement method in ASTM-D143-14 was used to calculate the key mechanical properties. The following conclusions are drawn:

(1) The tensile test of eight groups of bamboo scrimber-steel splints connections was studied. It was found that in the specimens that met the design specification size, accompanied by the shear and splitting failure of the main component and the crushing of the bolt holes, the yield mode of the bolts was Johansen’s yield mode IV. The shear failure of the bolts mostly occurred in the specimen group with large single bolt connection edge distance and multi-bolt spacing, and the bolts were sheared at the end of the bolts farther away from the loading end.

(2) In the single bolt connection, with the increase of bolt edge distance, the yield load and ultimate load of single bolt specimen increase first and then stabilize, and even the ultimate load decreases slightly with the increase of edge distance. The initial stiffness and ductility ratio tend to be stable as the edge distance increases.

(3) In the double bolt connection, with the increase of bolt spacing, the yield load and ultimate load gradually increase, and reach the maximum at the spacing of 6D, and then remain stable after a slight decrease. The yield displacement and ultimate displacement also reach the maximum at 6D, and a sudden decrease will occur when the spacing increases. The initial stiffness and ductility ratio remain stable with the change of spacing.

(4) The shear force prediction formulas of NDS, CSA and GB/T50005-2017 are too conservative in this paper, while the maximum error between the predicted load and the test load of Eurocode5 is only 11.97%. In this paper, based on Johansen’s yield mode IV and considering the rope effect and the group bolt effect, the shear bearing capacity formula of the bolted connection of the bamboo scrimber steel splint is proposed, and the theoretical value is in good agreement with the experimental value.

Acknowledgement

The writers gratefully acknowledge Dong Yang, Xin Xue, Yue Chen, and others from the Nanjing Forestry University for assisting in various capacities.

Funding Statement

This work was supported by the National Natural Science Foundation of China (No. 51878354 & 51308301); the Natural Science Foundation of Jiangsu Province (No. BK20181402 & BK20130978); 333 high-level talent projects of Jiang-su Province; and Qinglan Project of Jiangsu Higher Education Institutions. All research outcomes presented in this paper are those of the writer(s) and do not necessarily reflect the views of the foundations.

CRediT authorship contribution statement

Haitao Li: Conceptualization, Funding acquisition, Supervision, Investigation, Formal analysis, Writing - original draft. **Yougui Luo:** Investigation, Formal analysis, Writing - original draft. **Yijia Guo:** Investigation, Formal analysis, Writing – original draft. **Yukun Tian:** Writing-review & editing. **Chungui Zhou:** Investigation, Writing-review & editing.

Conflicts of Interest

The authors declare that they have no conflicts of interest to this work.

Data Availability Statement

The datasets generated and analysed during the current study are available from the corresponding author on reasonable request.

References

[1] P. Dietsch, R. Brandner, Self-tapping screws and threaded rods as reinforcement for structural timber elements – A state-of-the-art report, Construction and Building Materials 2015; 97: 78-79. https://doi.org/10.1016/j.conbuildmat.2015.04.028.
[2] J. Zhang, Y. Zhong, R. Zhao, H. Zhou, Reviews of Mechanical Properties for Timber Bolted Joints, Chinese Journal of Wood Science and Technology 2012; 26 : 39-42+52. https:// doi.org/10.19455/j.mcgy.2012.04.011.
[3] A. Hassanieh, H.R. Valipour, M.A. Bradford, Experimental and analytical behaviour of steel-timber composite connections, Construction and Building Materials 2016; 118: 63–75. https://doi.org/10.1016/j.conbuildmat.2016.05.052.
[4] A. Dauletbek, X. Xue, X. Shen, H. Li, Z. Feng, R. Lorenzo, K. Liu, E. Zea Escamilla, L. Yao, X. Zheng, Lightweight bamboo structures - Report on 2021 International Collaboration on Bamboo Construction, Sustain. Struct. 2023; 3(1): 000025. https://doi.org/10.54113/ j.sust.2023.000025.
[5] AKT II Ltd, L. Mimendi, R. Lorenzo, University College London, H. Li, College of Civil Engineering, Nanjing Forestry University, An innovative digital workflow to design, build and manage bamboo structures, Sustain. Struct. 2022; 2(1): 000015. https://doi.org/10.54113/ j. sust.2022.000011.
[6] Y. Chen, Experimental evaluation of the dowel-bearing strength of laminated flattened-bamboo lumber perpendicular to grain, Construction and Building Materials. 2022; 350: 128791. 10.1016/j.conbuildmat.2022.128791
[7] A. Kumar, T. Vlach, L. Laiblova, M. Hrouda, B. Kasal, J. Tywoniak, P. Hajek, Engineered bamboo scrimber: Influence of density on the mechanical and water absorption properties, Construction and Building Materials 2016; 127: 815–827. https://doi.org/10.1016/ j. conbuildmat.2016.10.069.
[8] H. Li, G. Wu, Q. Zhang, A.J. Deeks, J. Su, Ultimate bending capacity evaluation of laminated bamboo lumber beams, Construction and Building Materials 2018; 160: 365–375. 10.1016/j.conbuildmat.2017.11.058
[9] T. Wang, Y. Wang, R. Crocetti, M. Wålinder, In-plane mechanical properties of birch plywood, Construction and Building Materials 2022; 340: 127852. https://doi.org/10.1016/ j. conbuildmat.2022.127852.
[10] J.H. Quenneville, M. Mohammad. On the failure modes and strength of steel-wood-steel bolted timber connections loaded parallel-to-grain, Can. J. Civ. Eng. 2000; 27: 761–773. https://doi.org/10.1139/l00-020.
[11] X. Xue, W. Zhou, U. Sayed, Z. Feng, H. Li, Y. Li, Z. Huang, M. Ashraf, R. Lorenzo, Design and construction of "Bamboo Cubic" facade with laminated bamboo lumber, Sustain. Struct. 2023; 3(2): 000030. https://doi.org/10.54113/j.sust.2023.000030.
[12] J. Su, H. Li, Z. Xiong, R. Lorenzo, Structural design and construction of an office building with laminated bamboo lumber, Sustain. Struct. 2021; 1(2): 000010. https://doi.org/10.54113/j. sust. 2021.000010.
[13] G.W. Trayer, The bearing strength of wood under bolts, US Department of Agriculture, 1932.
[14] D.V. Doyle, Performance of joints with eight bolts in laminated douglas-fir, U.S. Dept. of Agriculture, Forest Service, Forest Products Laboratory, Madison, Wis., 1964.
[15] L.A. Soltis, F.K. Hubbard, T.L. Wilkinson, Bearing Strength of Bolted Timber Joints, Journal of Structural Engineering 1986; 112: 2141–2154. https://doi.org/10.1061/(ASCE)0733-9445(1986)112:9(2141).
[16] K.W. Johansen, Theory of timber connections, IABSE Publications = Mémoires AIPC = IVBH Abhandlungen 1949; 9: 249. https://doi.org/10.5169/seals-9703.
[17] L. Daudeville, L. Davenne, M. Yasumura, Prediction of the load carrying capacity of bolted timber joints, Wood Science and Technology 1999; 33: 15–29. https:// doi.org/10.1007/ s002260050095.
[18] M. Yasumura, Ultimate properties of bolted joints in glued-laminated timber, in: Proceedings of the CIB-W18 Meeting, Dublin, 1987, 1987.
[19] J.M. Cabrero, M. Yurrita, Performance assessment of existing models to predict brittle failure modes of steel-

to-timber connections loaded parallel-to-grain with dowel-type fasteners, Engineering Structures 2018; 171: 895–910. https://doi.org/10.1016/ j.engstruct.2018.03.037.
[20] Li X., Research on bearing performance of bolt joint for bamboo scrimber, Doctor, Chinese academy of forestry sciences, 2014. https://doi.org/10.7666/d.Y2405233 (accessed January 26, 2024).
[21] Ministry of Housing and Urban-Rural Development of China.Testing methods for physical and mechanical properties of bamboo used in building: JG/T 199—2007. Beijing:China Standard Press, 2007., (n.d.).
[22] A. D143-14, Standard test methods for small clear specimens of timber, ASTM International: West Conshohocke, PA, USA (2014).
[23] American Society for Testing and Materials, Standard test method for evaluatingdowel-bearing strength of wood and wood-based products, 2013. ASTM D576497a., (n.d.).
[24] American Forest and Paper Association (AF&PA), National Design Specification for Wood Construction.Washington DC: American Wood Council 2017., (n.d.).
[25] S. Liu, D. Gao, B. Chen, Experimental investigation on Steel-Bamboo Composite shear connections, Journal of Building Engineering. 2022; 61: 105207. https://doi.org/10.1016/j.jobe.2022.105207
[26] Canadian Standard Association (CSA). Engineering design in wood[S]. Mississauga, Ontario, Canada, 2009., (n.d.).
[27] The European Standard EN 1995-1-1: 2014(E), Eurocode 5: Design of Timber Structures-Part 1-1: General-common rules and rules for buildings; 2014., (n.d.).
[28] Cui Z., Experimental and theoretical research on fire resistance of steel-to-laminated bamboo bolted connections with slotted-in steel plates, Doctor, Southeast university, 2022. https://doi.org/10.27014/d.cnki.gdnau.2020.002924.
[29] Ministry of Construction, PRC. GB 50005-2017. Standard for design of timber structures. 2017., (n.d.).
[30] J.J. Zahn, Design Equation for Multiple-Fastener Wood Connections, Journal of Structural Engineering 1991; 117: 3477–3486. https://doi.org/10.1061/(ASCE)0733-9445(1991)117: 11(3477).